

# Research on the Performance of Magnetorheological Semi-Active Suspension with Stepped By-Pass Valve based on Fuzzy PID Control

Chenguang Yang<sup>1</sup>, Xiaolong Yang<sup>1\*</sup>, and Youming Zhou<sup>2</sup>

<sup>1</sup>School of Mechanical and Automotive Engineering, Guangxi University of Science and Technology, Liuzhou 545006, China

<sup>2</sup>Dongfeng Liuzhou Motor CO., LTD, Liuzhou 545006, China

(Received 30 July 2022, Received in final form 29 June 2023, Accepted 13 July 2023)

**At present, most of the seat suspensions of heavy-duty trucks use passive suspension and active suspension. The passive suspension has gradually failed to meet people's needs in terms of vibration reduction performance, and the active suspension will consume too much energy. In this paper, a stepped by-pass valve magnetorheological semi-active suspension based on fuzzy PID control is proposed. The Simulink is used to simulate the system. In the case of sinusoidal excitation, the results show that this semi-active suspension reduces the vertical acceleration by 44.36%, the dynamic deflection of the suspension by 29.63% and the dynamic deformation of the tire by 43.78% compared with the passive suspension. Under the condition of C-level road surface input, the vertical acceleration of the suspension is reduced by 35.14%, the dynamic deflection of the suspension is reduced by 31.93%, and the dynamic deformation of the tire is reduced by 27.65%.**

**Keywords :** magnetorheological semi-active suspension, stepped by-pass, fuzzy PID control, simulation analysis

## 1. Introduction

In the working environment of most construction machinery and heavy trucks, drivers and passengers are exposed to low-frequency and high-intensity vibrations, which cause serious harm to their health [1, 2]. This requires heavy-duty trucks to have better performance in terms of running comfort and stability. At present, passive suspension and air suspension are mostly used in heavy truck seat suspension, but the vibration reduction performance of passive suspension is not good, and air suspension will consume too much energy [3-5]. Therefore, semi-active suspensions using magnetorheological dampers have become the focus of researchers.

Dal-Seong Yoon *et al.* derived the nonlinear motion control equations for the semi-active suspension model and built a robust sliding mode controller (RSMC) for heave, roll and pitch motions. The response time of the magnetorheological damper is tested, and the results show that the performance of the semi-active suspension is better than that of the passive suspension regardless of the speed of the response time [6]. J. Yang *et al.* introduced a

negative stiffness mechanism into the design of a semi-active magnetorheological suspension, aiming to improve its vibration reduction performance to the level that an active suspension can achieve. Compared to passive suspension, sprung acceleration is reduced by 52.6% at low speeds and 29.7% at high speeds [7]. Carlos A. Duchanoy *et al.* propose a new hybrid magnetorheological damper model that combines a first-principles dynamic model with a deep neural network-based phenomenological model [8]. Xian-Xu and Sen Yang investigated a magnetorheological energy absorber-based semi-active seat suspension system designed to minimize damage and discomfort to the spine from shock and vibration caused by terrain or explosions [9]. Narwade, P *et al.* proposed that in order to improve the comfort level of passengers, it can be optimized for different road conditions to improve the ride comfort of vehicles [10].

It can be seen that in recent years, researchers have noticed that in the overall performance of the semi-active suspension system, not only the appropriateness of the control strategy, but also the influence of the magnetorheological damper on the overall performance of the suspension system should be considered. The first problem to be considered is the nonlinear characteristics of the magnetorheological fluid. The establishment of the mathematical model of the magnetorheological damper is

©The Korean Magnetism Society. All rights reserved.

\*Corresponding author: Tel: +8618307721513

Fax: +8618307721513, e-mail: yangxiaolong@gxust.edu.cn

carried out. In this paper, the structure of the stepped magnetorheological damper made by the laboratory is analyzed. The structured forward model of the magnetorheological damper is deduced by using the Bingham characteristic of the magnetorheological fluid, and the parameters of the polynomial inverse model are fitted by the experimental data. The overall simulation of the semi-active suspension system is carried out using the fuzzy PID control strategy to test the overall performance of the suspension system.

## 2. 2-DOF Magnetorheological Semi-Active Suspension System Model

This paper uses a simplified 1/4 car 2-DOF magnetorheological semi-active suspension system model as shown in Fig. 1. Where  $m_s$  is the sprung mass, which is 345 kg in this paper, and its corresponding vertical displacement after the suspension is excited is represented by  $z_s$ ,  $m_u$  is the unsprung mass, its size is 40.5 kg in this paper, and its corresponding vertical displacement is  $z_u$ ,  $z_r$  is the road excitation displacement,  $k_s$  is the spring stiffness of the suspension system, which is 17000 N/m in this paper,  $k_t$  is the tire stiffness, which is 192000 N/m in this paper,  $F_\eta$  is the viscous damping force of the magnetorheological damper.  $F_c$  is the magnetic damping force of the magnetorheological damper.

The differential equation of this semi-active suspension system is as follows:

$$\begin{aligned} m_s \ddot{z}_s + k_s(z_s - z_u) + F_\eta + F_c &= 0 \\ m_u \ddot{z}_u - k_s(z_s - z_u) + k_t(z_u - z_r) - F_\eta - F_c &= 0 \end{aligned} \quad (1)$$

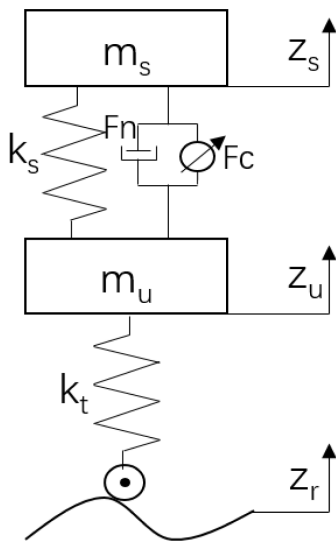


Fig. 1. 2-DOF magnetorheological semi-active suspension system model.

It can be seen from the above formula that the damping force is positive when the vehicle body and the wheels move in opposite outward directions. The damping force is divided into viscous damping force and magnetic damping force. The viscous damping force  $F_\eta$  is the fundamental damping force of the magnetorheological fluid in the absence of an external magnetic field. The magnetic damping force  $F_c$  is the additional damping force generated under the influence of an external magnetic field.

## 3. Mathematical Model of Stepped By-Pass Valve Magnetorheological Damper

### 3.1. Structural Forward Mathematical Model of Stepped By-Pass Valve Magnetorheological Damper

Under the action of an external magnetic field, the magnetorheological fluid will change from a static force state to a yielding flow process, and will have the characteristics of viscoelastic material before yielding, and the magnetorheological fluid will have characteristics similar to Bingham fluid after stable flow [11, 12]. The mathematical model of the stepped by-pass valve magnetorheological damper established in this paper uses the basic principle of the magnetorheological fluid Bingham model, and the damping force of the magnetorheological damper is represented by the viscous damping force and the magnetorheological damping force. The relationship is as follows:

$$F_D = F_\eta + F_c \quad (2)$$

The schematic diagram of the structure of the stepped by-pass magnetorheological damper used is shown in Fig. 2. The specific force analysis of the stepped by-pass valve magnetorheological damper is carried out, and the mathematical model of the damper that is closer to the actual situation is obtained.

Where  $F$  represents the external force on the piston rod,

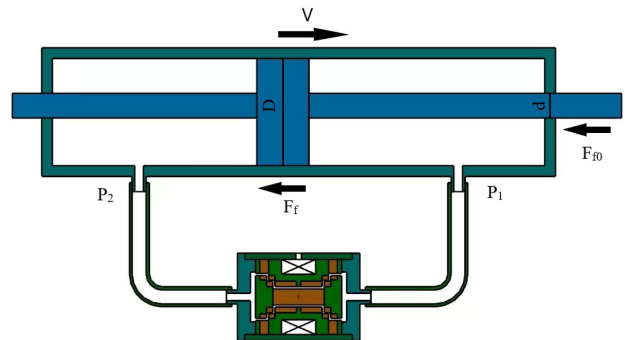


Fig. 2. (Color online) Structure diagram of stepped by-pass valve magnetorheological damper.

$F_D$  is the damping force generated by the damper,  $M$  represents the mass of the piston rod and piston head,  $D$  is the diameter of the piston head,  $d$  is the diameter of the piston rod, and  $x$  represents the displacement corresponding to the piston rod,  $A$  represents the contact area between the piston rod and the magnetorheological fluid,  $F_f$  is the friction between the piston head and the inner wall of the cylinder, and  $F_{f0}$  is the friction between the piston rod and the cylinder seal,  $P_1$  and  $P_2$  respectively represent the pressure values of the two ports of the bypass valve. The mechanical analysis of this damper can be obtained from Newton's second law:

$$F = M\ddot{x} + F_f + F_{f0} + (P_1A - P_2A)$$

$$A = \frac{\pi}{4}(D^2 - d^2) \quad (3)$$

$$F_D = F - M\ddot{x}$$

Since both  $F_f$  and  $F_{f0}$  belong to passive damping forces, the commonality between them is that they are related to the movement direction of the piston rod, and  $F_f \gg F_{f0}$ , so  $F_{f0}$  can be ignored:

$$F_D = F_f + (P_1A - P_2A) \quad (4)$$

According to the friction formula:

$$F_f = \mu F_K \quad (5)$$

In the formula,  $F_K$  is the positive pressure between the piston rod and the inner wall of the steel cylinder,  $\mu$  is the friction coefficient, and the coefficient value is not large, so this item can be ignored.

Therefore, the damping force formula can be written as (6):

$$F_D = P_1A - P_2A = \Delta PA \quad (6)$$

It can be known from the formula of the damping force that the magnitude of the damping force is mainly related to the contact area between the piston rod and the magnetorheological fluid, and the pressure difference

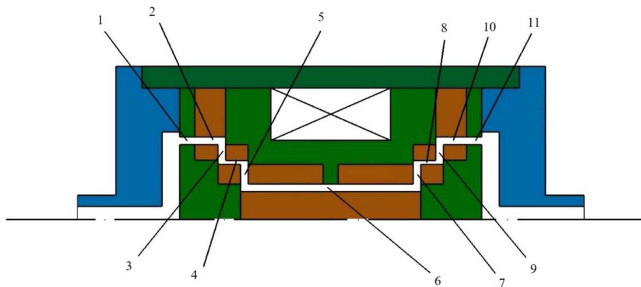


**Fig. 3.** (Color online) Schematic diagram of the by-pass valve flow channel.

between the two ends. When the pressure difference between the two ends of the through valve increases, the damping force also increases. The pressure of the bypass valve is mainly related to the liquid flow channel. The flow channel of the by-pass valve is shown in Fig. 3. The blue color represents the end cover, the green color represents some mechanical parts around the magnetic conducting ring, and the brown color represents the magnetic conducting ring.

The by-pass valve of the damper used in this paper has annular and disc shapes. 1, 2, 4, 6, 8, 10, 11 are annular liquid flow channels. 3, 5, 7, and 9 are disc type liquid flow channels.

The formula for calculating the viscous pressure difference of the ring is:

$$\Delta P_i = \frac{6\mu L_i}{\pi R_i g_r^3} Q \quad (7)$$

The calculation formula of the magnetic pressure difference of the ring is:

$$\Delta P_{ic} = \frac{CL_i \tau_y}{g_r} \quad (8)$$

The formula for calculating the viscous pressure difference in the disc shape is:

$$\Delta P_{iz} = \frac{6\mu Q}{\pi g_z^3} \ln\left(\frac{R_{iz}}{R_{izr}}\right) \quad (9)$$

The calculation formula of the disc-shaped magneto-

**Table 1.** Damper related parameters.

Parameter	Size (mm)
Piston head diameter $D$	40
Piston rod diameter $d$	20
Lengths of annular liquid flow channels $L_1$ and $L_{11}$	4
Lengths of annular liquid flow channels $L_2$ and $L_{10}$	6
Lengths of annular liquid flow channels $L_4$ and $L_8$	6
Lengths of annular liquid flow channels $L_6$	33
Inner radius of annular liquid flow channel $R_1$ and $R_{11}$	26.5
Inner radius of annular liquid flow channel $R_2$ and $R_{10}$	26.5
Inner radius of annular liquid flow channel $R_4$ and $R_8$	20.5
Inner radius of annular liquid flow channel $R_6$	10.5
The thickness of the annular liquid flow channel $g_r$	1
Outer diameter of disc-shaped liquid flow channel $R_{3z}$ and $R_{9z}$	26
Outer diameter of disc-shaped liquid flow channel $R_{5z}$ and $R_{7z}$	20
Inner diameter of disc-shaped liquid flow channel $R_{3zr}$ and $R_{9zr}$	20
Inner diameter of disc-shaped liquid flow channel $R_{5zr}$ and $R_{7zr}$	10
The thickness of disc-shaped liquid flow channel $g_z$	1

induced pressure difference is:

$$\Delta P_{in} = \frac{C(R_{iz} - R_{izr})\tau_y}{g_z} \quad (10)$$

The used magnetic fluid is an ester-based magnetic fluid prepared by our group. The density and the saturation magnetization of magnetic fluid are  $1.32 \times 10^3 \text{ kg/m}^3$  and  $30.7 \text{ kAm}^{-1}$  respectively.

Where  $\mu$  is the viscosity of the magnetorheological fluid, the size in this article is  $0.8 \text{ Pa}\cdot\text{s}$ .  $Q$  is the flow rate through the ring, which is related to the speed of the piston head and can be measured experimentally,  $L_i$  is the length of the ring,  $g_r$  is the thickness of the ring, and  $g_z$  is the thickness of the disc,  $R_i$  is the inner radius of the ring,  $R_{iz}$  is the outer diameter of the disc,  $R_{izr}$  is the inner diameter of the disc, and  $C$  is a constant generally taken as 2-3. The damper parameters are shown in Table 1.

$\tau_y$  is the shear yield strength of the magnetorheological fluid, which is related to the magnetic field intensity. So  $\tau_y$  is a function of the control current  $I$ , the relationship is as (11):

$$\tau_y = A_1 e^{-1} + A_2 \ln(I + e) + A_3 I \quad (11)$$

Among them,  $A_1 = -11374$ ,  $A_2 = 14580$ ,  $A_3 = 1281$  are the coefficients related to the performance of magnetorheological variants, and  $e$  is a natural constant.

So far, the forward expression of the damping force of the stepped by-pass magnetorheological damper can be obtained as (12):

$$\begin{aligned} F_\eta &= [2(\Delta P_1 + \Delta P_2 + \Delta P_4 + \Delta P_{3z} + \Delta P_{5z}) + \Delta P_6] A \\ F_c &= [2(\Delta P_{1c} + \Delta P_{2c} + \Delta P_{4c} + \Delta P_{3n} + \Delta P_{5n}) + \Delta P_{6c}] A \end{aligned} \quad (12)$$

### 3.2. Polynomial Inverse Model of Stepped By-Pass Valve Magneto-Rheological Damper

In the semi-active suspension, the controller solves the problem according to the two feedback state quantities of the suspension vertical velocity and acceleration, outputs the expected damping force, and transmits this information to the magnetorheological damper to generate the damping force. However, the magnitude of the control current  $I$  affects the internal magnetic field strength of the magnetorheological damper, so that the yield effect of the magnetorheological fluid produces shear stress, so the expected damping force output by the controller should be converted into a current value and transmitted to the damper. This requires the establishment of an inverse model of the magnetorheological damper [13, 14]. The control current  $I$  must be obtained from the expected value of  $F_D$ .

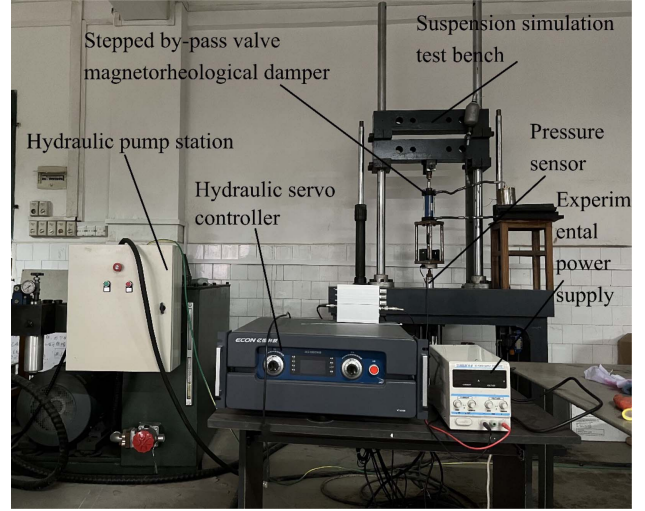


Fig. 4. (Color online) Experimental value of damping force under different currents.

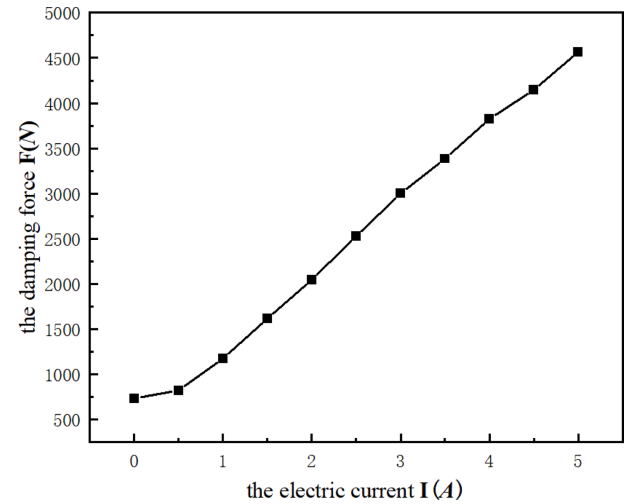


Fig. 5. Experimental value of damping force under different currents.

Because the relationship between the shear yield strength  $\tau_y$  of the magnetorheological fluid and the control current  $I$  has a strong nonlinearity, it is difficult to directly invert the relationship between the overall magnetorheological damper  $F_D$  and  $I$ . In this paper, a bench experiment is carried out on the stepped valve magnetorheological damper, and the experimental data between the damping force  $F_D$  and the control current  $I$  are obtained. The damper suspension experiment is shown in Fig. 4. The experimental results are shown in Fig. 5.

Perform data fitting on the experimental values of the damping force under different currents, use the fitting toolbox of Matlab, select the control current  $I$  as the y value, and the damping force as the x value, and use the

third-order polynomial fitting to finally obtain the relational parameters. Thus, the mathematical expression between  $I$  and  $F_D$  is obtained as (13):

$$I = P_1 F_D^3 + P_2 F_D^2 + P_3 F_D + P_4 \quad (13)$$

Where  $P_1 = 0.0000000005912$ ,  $P_2 = -0.0000004839$ ,  $P_3 = 0.002373$ ,  $P_4 = -1.315$ , so far, the forward model mathematics and the reverse mathematical model relationship of the stepped by-pass magnetorheological damper are known. Simply designing the appropriate controller allows the magnetorheological damper to generate damping forces in the semi-active suspension.

### 4. Design of Fuzzy PID Controller

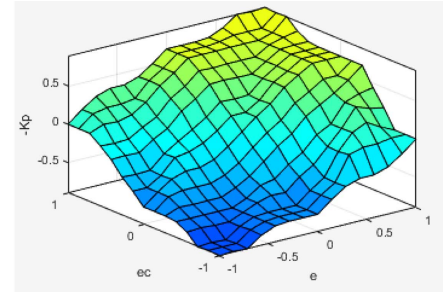
The fuzzy adaptive PID controller is formed by the combination of the fuzzy controller module and the PID control module. In the fuzzy controller, the vibration reduction effect of the suspension system is considered to be composed of multiple factors, and the vertical acceleration of the sprung mass is selected as the feedback state quantity, in order to improve the accuracy of the fuzzy rules, the difference between the state quantity and the ideal target and the change rate of the state difference are selected as the input of the fuzzy controller [15]. The specific schematic diagram is shown in Fig. 6.

The two input quantities of the fuzzy controller and the three outputs  $\Delta K_p, \Delta K_i, \Delta K_d$  of the fuzzy controller are described using 7 subsets of fuzzy language, i.e. {NB, NM, NS, ZO, PS, PM, OB}. After normalizing it, the interval is set to  $[-1, 1]$ . Then its fuzzy universe becomes  $\{-1, -0.833, -0.667, -0.5, -0.333, -0.167, 0, 0.167, 0.333, 0.5, 0.667, 0.833, 1\}$ . From this, the scale factor of the input quantity and the quantization factor of the output quantity can be calculated.

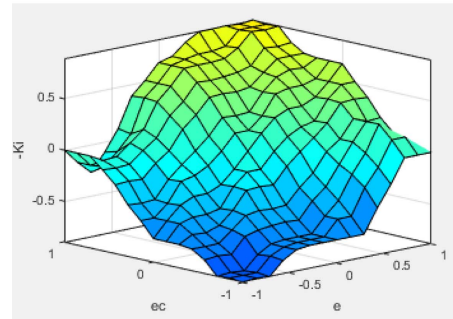
After establishing the membership function of the triangular function, 49 rules of fuzzy control of  $e$  and  $ec$  on  $\Delta k_p, \Delta k_i, \Delta k_d$  of the fuzzy controller can be written.

The membership function surface generated by the 49 fuzzy control rules is shown in Fig. 7.

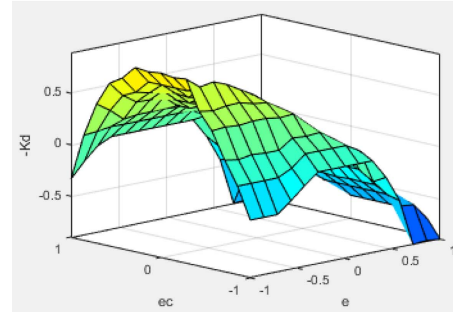
So far the fuzzy control module has been completed, the PID controller is adjusted and combined by the error



(I)



(II)



(III)

Fig. 7. (Color online) Surface view of membership function (I)  $\Delta k_p$  (II)  $\Delta k_i$  (III)  $\Delta k_d$ .

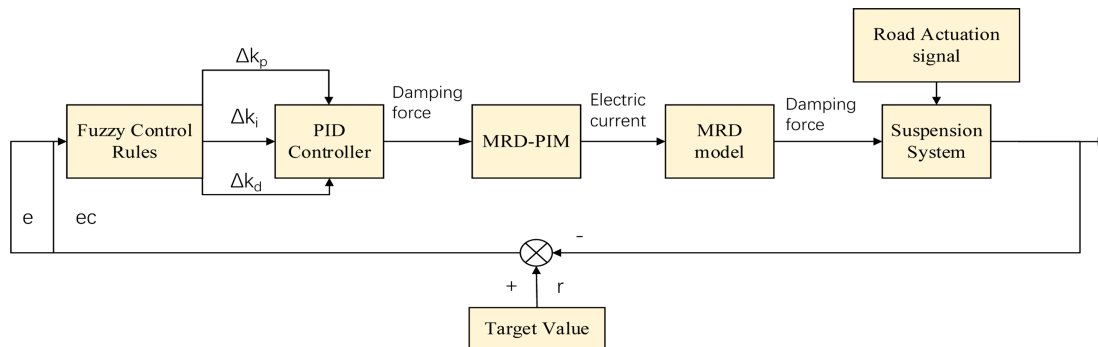
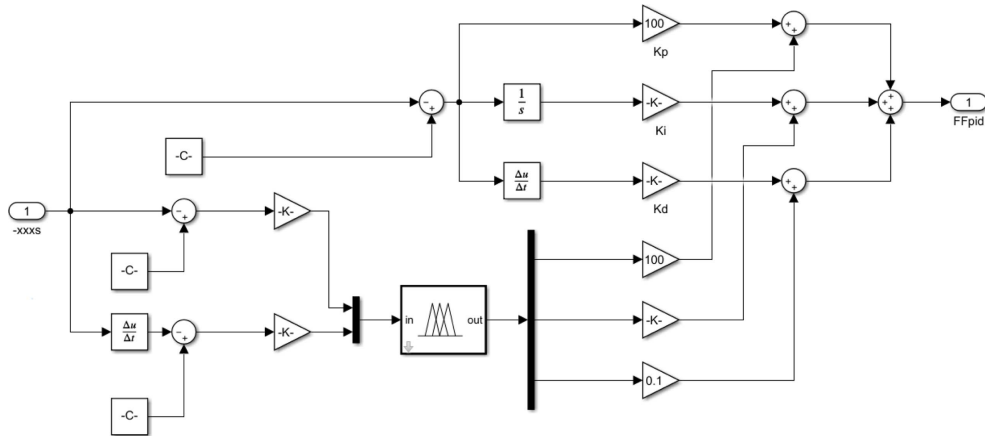


Fig. 6. (Color online) Structural diagram of magnetorheological semi-active suspension controller.



**Fig. 8.** Simulink simulation structure of fuzzy PID controller.

and the differential of the error and the integral of the error, and finally the controller output is obtained as equation (14).

$$u_{pid} = k_p e + k_i \int_0^t e dt + k_d \frac{de}{dt} \quad (14)$$

The Simulink simulation structure of the final fuzzy PID controller is shown in Fig. 8.

### 5. Simulation Analysis of Performance of Stepped By-Pass Valve Magnetorheological Semi-Active Suspension Based on Fuzzy PID Control

All the models have been designed, and the simulation model is built in Simulink. The simulation and comparison of the passive suspension and the stepped by-pass valve

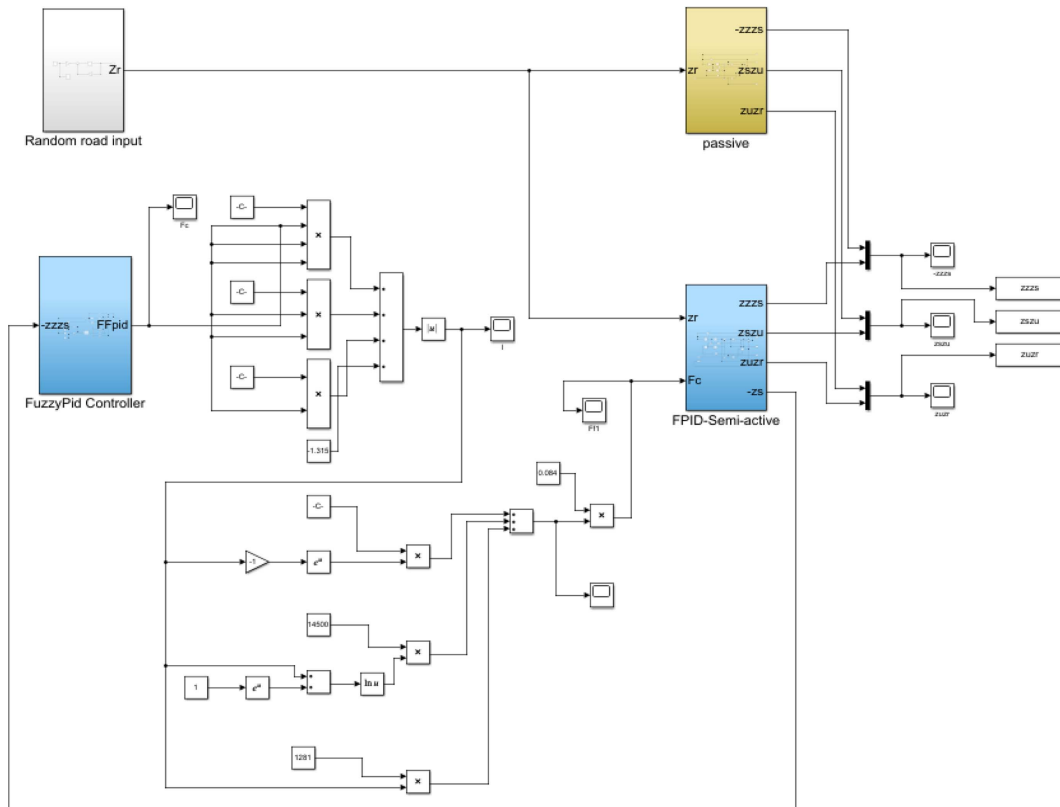


**Fig. 9.** (Color online) Simulink simulation model of stepped by-pass valve magnetorheological semi-active suspension based on fuzzy PID control.



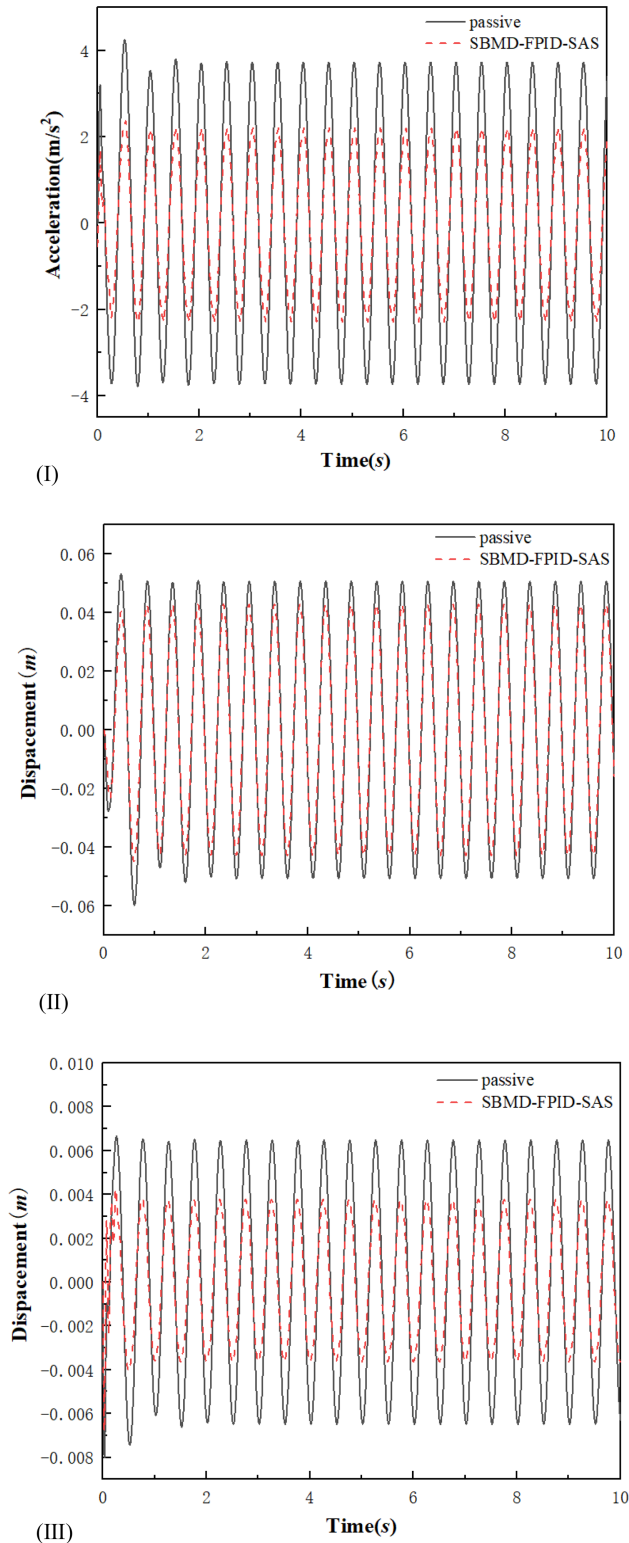


**Fig. 10.** (Color online) Performance comparison between passive suspension and magnetorheological semi-active suspension with stepped by-pass valve based on fuzzy PID control under sinusoidal excitation (I) Vertical acceleration of suspension (II) Dynamic deflection of suspension (III) Dynamic deformation of tire.

magnetorheological semi-active suspension based on fuzzy PID control are carried out. The simulation structure is shown in Fig. 9.

During the simulation, the random road excitation model and the positive selection excitation model are calculated for input, and the positive selection signal selects a sine wave with an amplitude of 0.04 m and a frequency of 2 Hz. The simulation results of the vertical acceleration of the suspension sprung mass, the dynamic deflection of the suspension and the dynamic deformation of the tire are shown in Fig. 10.

It can be seen from the simulation results in Fig. 10 that in the case of sinusoidal excitation, the use of the stepped bypass valve magnetorheological semi-active suspension based on fuzzy PID control improves the vibration reduction effect significantly compared with the passive suspension. By comparison, the vertical acceleration is reduced by 44.36%, the dynamic deflection of the suspension is also reduced by 29.63% compared with the passive suspension, and the dynamic deformation of the tire is reduced by 43.78%. It shows that the semi-active suspension is better than the passive suspension in vehicle ride comfort, and it also verifies that the mathematical model of the stepped by-pass valve magnetorheological damper is feasible.

During the simulation, a corresponding road surface mechanism model needs to be established to generate  $z_r$ . According to the random vibration theory, the road surface roughness can be regarded as a stable random process of Gaussian states ergodic when the vehicle is running at a constant speed. The power spectrum of road roughness can be expressed by equation (15):

$$G(n) = G_q(n_0) \left( \frac{n}{n_0} \right)^{-W} \quad (15)$$

In this paper, the filter white noise method is used to establish a time-domain random road excitation model. By combining the time domain expression of the first-order filtered white noise system with the time-frequency power spectral density [16], equation (16) can be obtained.

$$\begin{aligned} \dot{z}_r + 2\pi f_{\min} z_r &= 2\pi n_0 \sqrt{G_{xr}(n_0)} v W(t) \\ f_{\min} &= v n_{\min} \end{aligned} \quad (16)$$

where  $W(t)$  represents white Gaussian noise as the excitation,  $v$  is the vehicle speed,  $G_{xr}(n_0)$  is the road surface roughness coefficient,  $n_0$  is the reference spatial frequency,  $n_0 = 0.1 \text{ m}^{-1}$ ,  $n_{\min}$  is the lower limit cutoff frequency of the space, and  $n_{\min} = 0.011 \text{ m}^{-1}$ .

In this simulation study with random road surface as

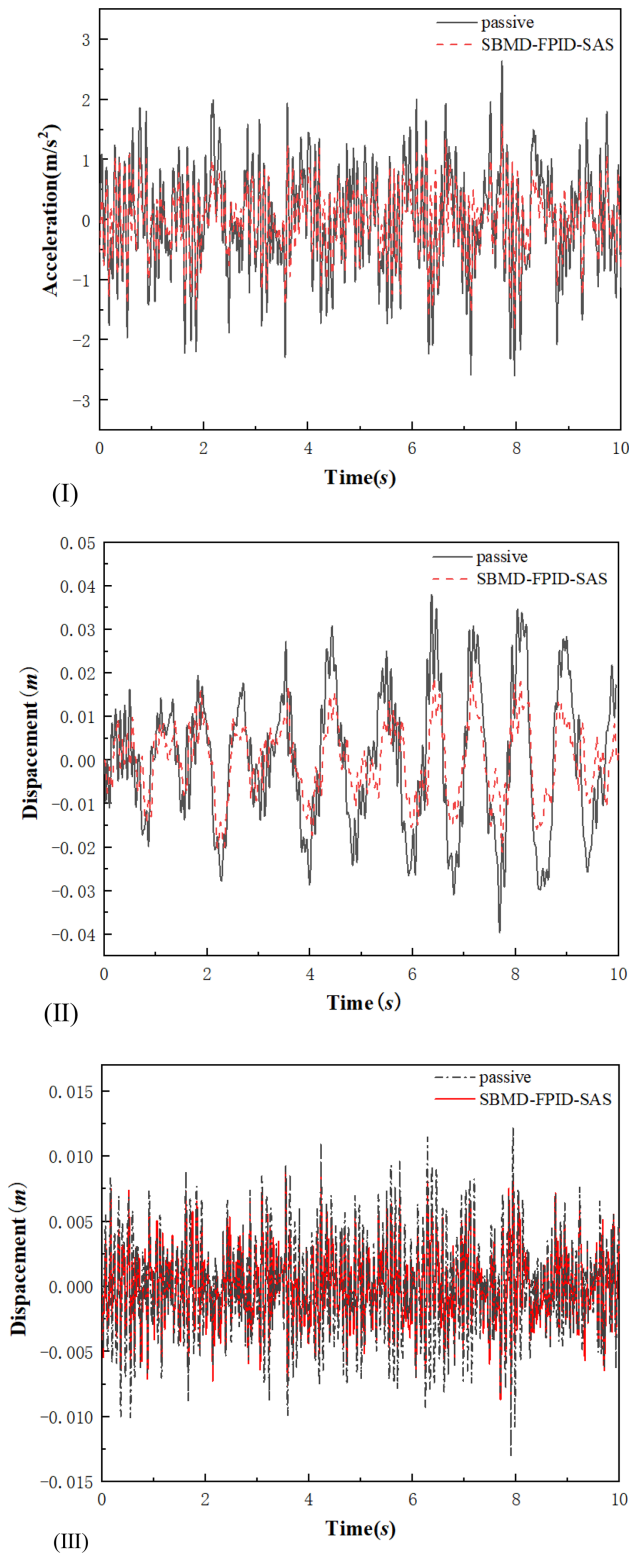


**Fig. 11.** (Color online) Performance comparison between passive suspension and magnetorheological semi-active suspension with stepped by-pass valve based on fuzzy PID control under random road surface excitation (I) Vertical acceleration of suspension (II) Dynamic deflection of suspension (III) Dynamic tire deformation.

input, the case where the speed of C-level road is 10 m/s is selected. The three aspects of suspension vertical acceleration, suspension dynamic deflection and tire dynamic deformation are simulated for the stepped bypass valve magnetorheological semi-active suspension based on fuzzy PID control and the passive suspension. The simulation results are shown in Fig. 11.

Calculated using the root mean square method on simulated data, under the condition of C-level road surface input, the stepped by-pass valve magnetorheological semi-active suspension based on fuzzy PID control reduces the vertical acceleration of the suspension by 35.14%, the dynamic deflection of the suspension by 31.93%, and the dynamic tire deformation is reduced by 27.65% compared with the passive suspension. According to the driving performance evaluation criteria, according to the simulation results of vertical acceleration of the suspension, this semi-active suspension greatly improves the ride comfort compared with the passive suspension. According to the simulation results of suspension dynamic deflection, this semi-active suspension is also greatly improved in handling stability and driving safety compared with passive suspension. According to the tire dynamic deformation simulation results, this semi-active suspension has stronger road adhesion than the passive suspension.

## 6. Conclusion

This paper takes the seat suspension vibration reduction problem as the research starting point. Structural analysis of stepped by-pass valve magnetorheological damper based on Bingham characteristics of magnetorheological fluid. A structural forward model of the magnetorheological damper that conforms to the design criteria is obtained. The relationship between the damping force and the current in the damper experiment was fitted, and the polynomial inverse model of the stepped by-pass valve magnetorheological damper was obtained, which was brought into the semi-active suspension model. The fuzzy PID control algorithm that has been widely used in various fields is selected, and the expected damping force of the suspension system is calculated for this magnetorheological damper, and the forward and inverse models of the damper are transmitted to make the damper generate appropriate damping force.

The stepped by-pass valve magnetorheological semi-active suspension based on fuzzy PID and passive suspension system are simulated and compared by using Simulink. Through the sinusoidal excitation simulation, it can be concluded that compared with the passive suspension, the magnetorheological semi-active suspension



reduces the vertical acceleration by 44.36%, the dynamic deflection of the suspension by 29.63%, and the dynamic deformation of the tire by 43.78%. After the C-level random road excitation simulation, the results show that the magnetorheological semi-active suspension reduces the vertical acceleration of the suspension by 35.14%, the dynamic deflection of the suspension by 31.93%, and the dynamic deformation of the tire by 27.65%. It can be seen that the stepped by-pass valve magnetorheological semi-active suspension based on fuzzy PID control has a great improvement in ride comfort, handling stability, driving safety and road adhesion compared with passive suspension.

### Acknowledgment

The authors gratefully acknowledge the support of the National Nature Science Foundation of China (Grant No. 51905114), the support of the Science and Technology Project of Guangxi Province (Grant No. 2020GXNSFAA 159042), and the support of the Science and Technology Project of LiuZhou (Grant No. 2017BC20204).

### References

- [1] X. M. Du, M. Yu, J. Fu, and C. Q. Huang, *Smart Mater. Struct.* **7**, 29 (2020).
- [2] A. Heidarian and X Wang, *Applied Sciences* **14**, 9 (2019).
- [3] A. M. A. Soliman and M. M. S. Kaldas, *J. Low Freq. Noise V A.* **2**, 40 (2021).
- [4] H. Pang, F. Liu, and Z. Xu, *Neurocomputing* **306**, 130 (2018).
- [5] A. S. Yıldız and S. Sivrioğlu, *Asian J. Control.* **3**, 1380 (2021).
- [6] D. S. Yoon, G. W. Kim, and S. B. Choi, *Mech. Syst. Signal Pr.* **146**, 106999 (2021).
- [7] J. Yang, D. Ning, and S. S. Sun, *Mech. Syst. Signal Pr.* **147**, 107071 (2021).
- [8] C. A. Duchanoy, M. A. Moreno-Armendáriz, J. C. Moreno-Torres, and C. A. Cruz-Villar, *Sensors* **6**, 1333 (2019).
- [9] X. X. F. Bai and S. Yang, *J. Intel. Mat. Syst. Str.* **11**, 1613 (2019).
- [10] P. Narwade, R. Deshmukh, and M. Nagarkar, *J. Vib. Eng. Technol.* **1**, 8 (2022).
- [11] X. Jiang, J. Wang, and H. Hu, *J. Cent. South Univ.* **7**, 1839 (2012).
- [12] M. H. Jamadar, R. M. Desai, and R. S. T. Saini, *J. Vib. Eng. Technol.* **1**, 161 (2021).
- [13] T. Ma, F. Bi, X. Wang, C. Tian, J. Lin, and G. Peng, *Energies.* **6**, 1674 (2021).
- [14] L. H. Zong, X. L. Gong, and C. Y. Guo, *Vehicle Syst. Dyn.* **7**, 1025 (2012).
- [15] A. G. A. Muthalif, H. B. Kasemi, and N. H. D. Nordin, *Smart Struct. Syst.* **1**, 85 (2017).
- [16] R. S. Prabakar, C. Sujatha, and S. Narayanan, *J. Sound Vib.* **3**, 400 (2009).